The Subcritical Collapse of Predator Populations in Discrete-Time Predator–Prey Models

MICHAEL G. NEUBERT AND MARK KOT
Department of Applied Mathematics, FS-20,
University of Washington, Seattle, Washington 98195

Received 15 August 1991; revised 18 December 1991

ABSTRACT

Many discrete-time predator–prey models possess three equilibria, corresponding to (1) extinction of both species, (2) extinction of the predator and survival of the prey at its carrying capacity, or (3) coexistence of both species. For a variety of such models, the equilibrium corresponding to coexistence may lose stability via a Hopf bifurcation, in which case trajectories approach an invariant circle. Alternatively, the equilibrium may undergo a subcritical flip bifurcation with a concomitant crash in the predator's population. We review a technique for distinguishing between subcritical and supercritical flip bifurcations and provide examples of predator–prey systems with a subcritical flip bifurcation.

1. INTRODUCTION

Simple nonlinear difference equations,

$$N_{t+1} = f(N_t), \tag{1}$$

are commonly used to model the growth of populations with discrete, nonoverlapping generations. Models of this type have a long history and are known to possess complicated dynamics [27, 28].

The coupled dynamics of a predator and prey may, in turn, be modeled as a system of first-order difference equations:

$$N_{t+1} = f(N_t, P_t), \tag{2a}$$

$$P_{t+1} = g(N_t, P_t). \tag{2b}$$

Such systems are especially relevant to the study of arthropod predator–prey and host–parasitoid interactions [12], but they also appear in mathematics

655 Avenue of the Americas, New York, NY 10010 0025-5564/92/$5.00

and physics literature as mappings of the plane or as idealized Poincaré maps [2, 10, 14].

Nicholson and Bailey [34, 35] pioneered the use of discrete-time host–parasitoid models. They assumed density-independent growth of the host, a linear functional response, and random encounters between the host and the parasitoid. Their equations exhibit growing oscillations for all plausible parameter values. In contrast, many natural systems maintain coexistence at an equilibrium. Moreover, a stable equilibrium is the goal of many biological control programs [8]. As a result, there has been considerable interest in the factors that affect the stability of host–parasitoid or predator–prey equilibria, factors such as density dependence, functional response, age structure, spatial heterogeneity, and aggregation [4, 5, 12, 13, 31, 33, 44].

A number of discrete-time predator–prey models possess three fixed points or equilibria that correspond to (1) extinction of both species, (2) extinction of the predator with survival of the prey at its carrying capacity, and (3) coexistence of both species. In Section 3 of this paper, we consider the stability of the equilibrium of coexistence as it arises in a discrete-time Lotka–Volterra model. In Sections 4 and 5, we use simple linear stability analysis, center manifold theory, and bifurcation theory to examine the various ways in which this fixed point loses its stability. We highlight an "unexpected" subcritical flip bifurcation that produces a crash in the predator's population. The same bifurcation occurs in at least three other, equally well-known models. These are presented in Section 6. We relegate our concluding comments to Section 7.

The models we study have been in the literature for some time. It is not our aim to exhaustively review them. Instead, we wish to remind the reader that a linear analysis is not always sufficient to illuminate the nature of a bifurcation. In particular, there is a tendency to assume that all flip bifurcations are supercritical, that they will always produce a stable 2-cycle in the vicinity of the now unstable equilibrium. We show that this is false for four simple predator–prey models.

2. THE MODEL

Early on, Lotka [25] and Volterra [43] proposed the simple predator–prey model

$$\frac{dN}{dt} = rN\left(1 - \frac{N}{K}\right) - eNP, \tag{3a}$$

$$\frac{dP}{dt} = bNP - dP, \tag{3b}$$

where N and P are the densities of the prey and predator populations,

respectively. The parameters r and K are the intrinsic rate of growth and the carrying capacity of the prey; e, b, and d measure the foraging efficiency, the birth rate, and the death rate of the predator. The equations

$$N_{t+1} = N_t + rN_t\left(1 - \frac{N_t}{K}\right) - eN_tP_t, \tag{4a}$$

$$P_{t+1} = bN_tP_t + (1-d)P_t, \tag{4b}$$

first studied by Maynard Smith [30], are a discrete-time analog of (3). They are obtained by replacing the derivatives in (3) with divided differences,

$$\frac{dN}{dt} \approx \frac{N_{t+h} - N_t}{h}, \qquad \frac{dP}{dt} \approx \frac{P_{t+h} - P_t}{h}, \tag{5}$$

by scaling the generation time h to 1, and by forcing predators to die after one generation ($d = 1$). After rescaling Equations (4) via

$$x_t = N_t/K, \qquad y_t = eP_t/bK, \qquad \text{and} \quad c = bK, \tag{6}$$

we obtain

$$x_{t+1} = (r+1)x_t - rx_t^2 - cx_ty_t, \tag{7a}$$

$$y_{t+1} = cx_ty_t. \tag{7b}$$

This mapping has the undesirable property that it may generate negative numbers of individuals. However, the simple algebraic form of (7) greatly facilitates its analysis in comparison with those models that do preserve first-quadrant invariance. Other models, of both classes, are discussed in Section 7.

3. STABILITY ANALYSIS

The three fixed points of (7) and the eigenvalues associated with each are summarized in Table 1. X^* will be referred to as the "coexistence equilibrium." It is of fundamental interest to know if there is a region in

TABLE I

Fixed Points and Associated Eigenvalues of the Discrete-Time Lotka–Volterra Model

Fixed points	Eigenvalues
$X^0 = (0,0)$	$\lambda_1^0 = r+1, \quad \lambda_2^0 = 0$
$X^1 = (1,0)$	$\lambda_1^1 = 1-r, \quad \lambda_2^1 = c$
$X^* = \left(\frac{1}{c}, \frac{r(c-1)}{c^2}\right)$	$\lambda_{1,2}^* = 1 - \frac{1}{2c}\left\{r \pm \left[r^2 + 4rc(1-c)\right]^{1/2}\right\}$

parameter space [the (c, r) plane] for which this equilibrium is locally stable (i.e., has eigenvalues of magnitude less than 1). The easiest way to determine such a region is to apply the Jury conditions [17] to the community matrix [the Jacobian of (7) evaluated at X^*],

$$J(X^*) = \begin{pmatrix} 1 - rc & -1 \\ r - r/c & 1 \end{pmatrix}. \tag{8}$$

There are three ways that an eigenvalue may exit the unit circle in the complex plane, and, in this instance, there are three Jury conditions:

$$1 - \operatorname{tr} J(X^*) + \det J(X^*) > 0, \tag{9a}$$

$$1 + \operatorname{tr} J(X^*) + \det J(X^*) > 0, \tag{9b}$$

$$1 - \det J(X^*) > 0. \tag{9c}$$

The first two conditions guarantee that real eigenvalues larger than $+1$ or less than -1 do not exist. The third precludes truly complex eigenvalues from lying outside the unit circle. When these conditions are applied to (8), the following region in parameter space (Figure 1) is found to admit a

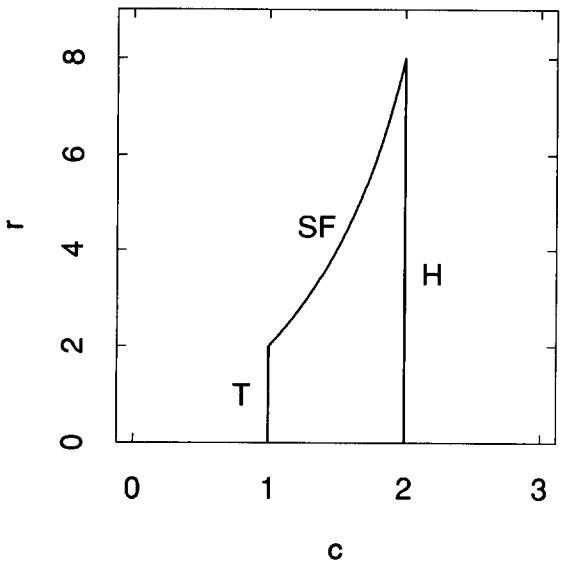

FIG. 1. The region of the parameter plane corresponding to the stability of the coexistence equilibrium X^* of models (7) and (26). X^* loses its stability via a transcritical, subcritical flip, or Hopf bifurcation as the boundaries labeled **T**, **SF**, or **H** are traversed.

locally stable X^*:

$$1 < c < 2, \tag{10}$$

$$r < 4c/(3-c). \tag{11}$$

4. LOCAL BIFURCATIONS

At the boundary **T** in Figure 1, we observe a transcritical bifurcation. X^* moves from the fourth to the first quadrant; it passes through and exchanges stability with X^1 (Figure 2). In effect, an increase in the predator's birth rate or the prey's carrying capacity allows the predator to invade the system.

As we continue to increase c, we observe a Hopf bifurcation (Figures 1 and 3). To the left of **H**, X^* is a stable focus. To the right of **H**, we observe an unstable focus and an attracting invariant circle. This Hopf bifurcation is an example of Rosenzweig's [39] paradox of enrichment [24]: we destabilize the predator–prey steady state by increasing the prey's carrying capacity. There are two exceptions to this Hopf bifurcation. They occur at $r = 4$ and $r = 6$, where there are strong 1:4 and 1:3 resonances (cf. [16], [21]). At $r = 4$, the eigenvalues of X^* are fourth roots of unity. X^* yields to a stable 4-cycle. At $r = 6$, the eigenvalues are third roots of unity,

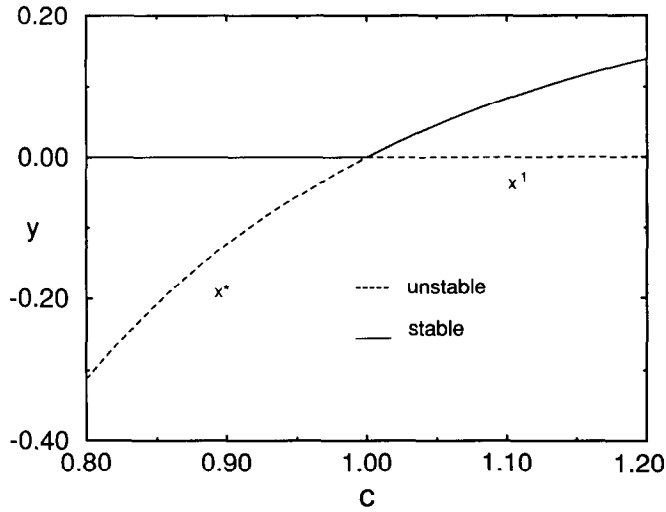

FIG. 2. Bifurcation diagram showing a transcritical bifurcation between X^* and X^1 in model (7). Predator numbers are plotted for $r = 1$ and various values of the parameter c.

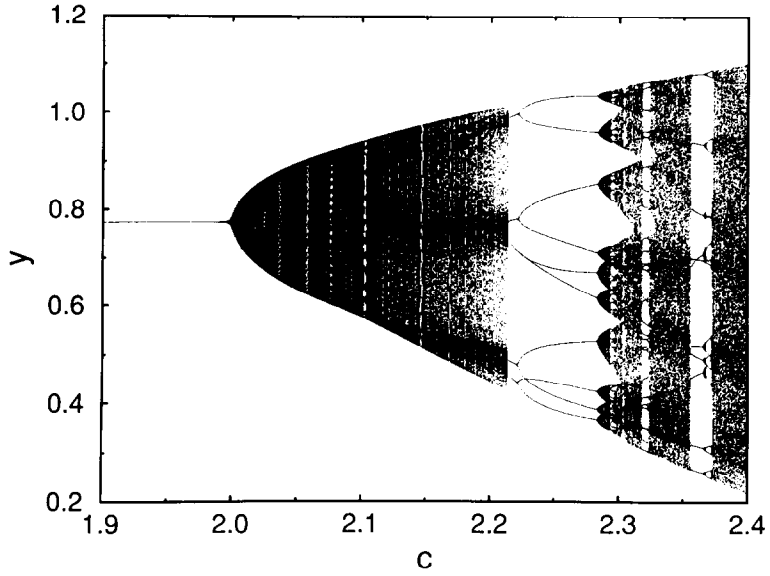

FIG. 3. Bifurcation diagram showing a Hopf bifurcation of X^* in model (7). For $r = 3.1$ and for each of 1000 values of c in the range 1.9–2.4, we allowed 1000 convergence iterations and plotted predator numbers from the next 350 iterates. Other bifurcations (including secondary Hopf bifurcations) can be seen for larger values of c.

and we observe an unstable 3-cycle. For larger values of c, the invariant circle generated by the Hopf bifurcation deforms and breaks apart, giving rise to a strange attractor (Figure 4). This breakup has been studied in detail for related discrete-time mappings [2, 3, 32].

If the intrinsic rate of growth of the prey becomes large and (11) is violated, the bifurcation behavior of X^* is more complicated (Figure 5). We focus here on the situation for small $c \approx 1.1$. As r increases, the fixed point X^1 goes through the series of period-doubling bifurcations that is the hallmark of the logistic map [27, 28]. The first such period doubling gives rise to the 2-cycle

$$\hat{X} = \{\hat{X}_1, \hat{X}_2\}, \tag{12a}$$

$$\hat{X}_1 = \left(\frac{r+2-\sqrt{r^2-4}}{2r}, 0\right), \tag{12b}$$

$$\hat{X}_2 = \left(\frac{r+2+\sqrt{r^2-4}}{2r}, 0\right). \tag{12c}$$

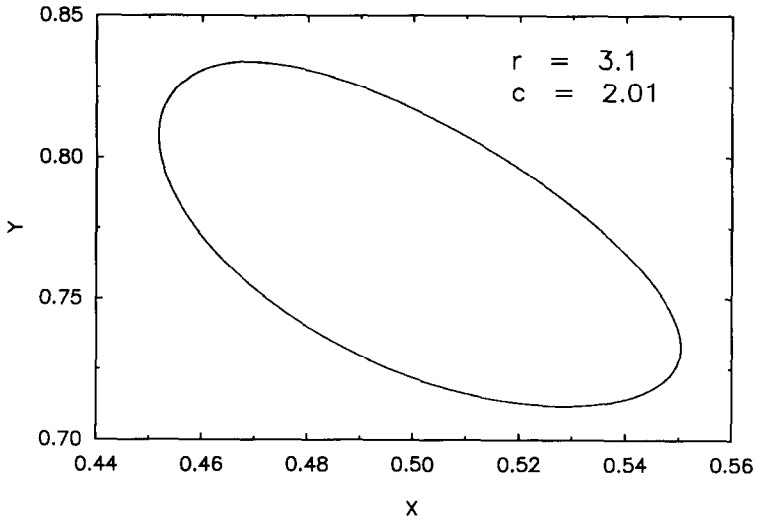

(a)

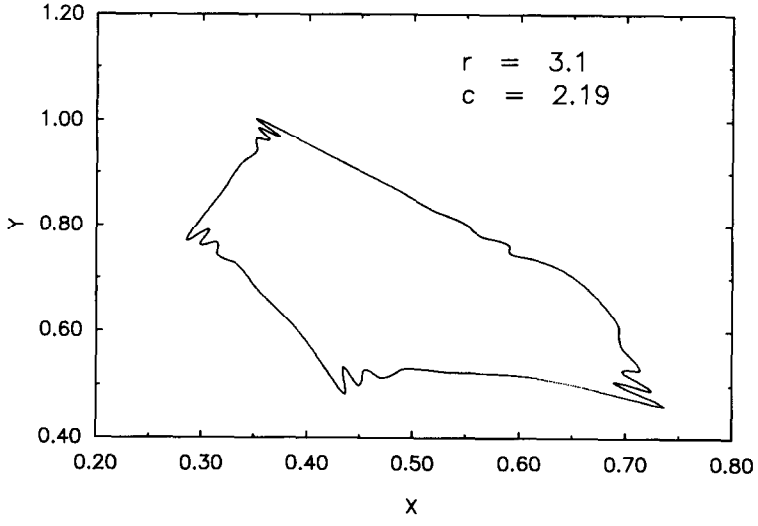

(b)

FIG. 4. Collapse of an invariant circle. System (7) was iterated 10,000 times, after a transient of 1000 iterations, for the initial conditions ($x_0 = 0.5$, $y_0 = 0.8$). As c increases, the invariant circle (a), which resulted from a Hopf bifurcation, becomes kinked (b), locks into a 10-cycle, undergoes a secondary Hopf bifurcation (c), and eventually becomes a strange attractor (d).

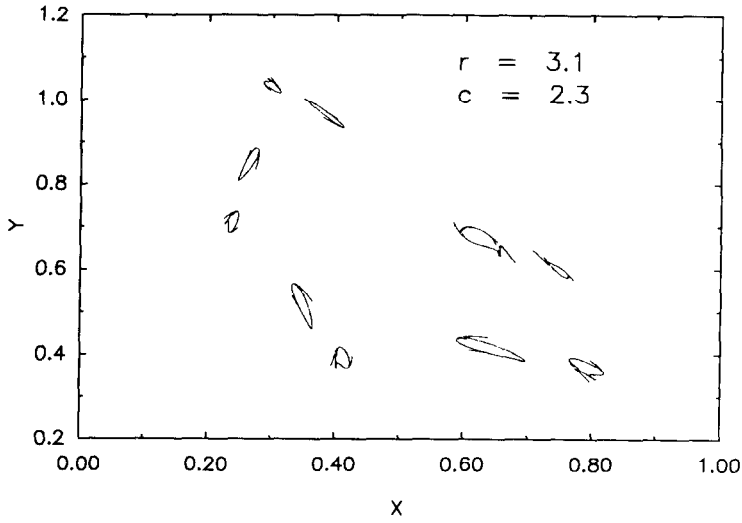

(c)

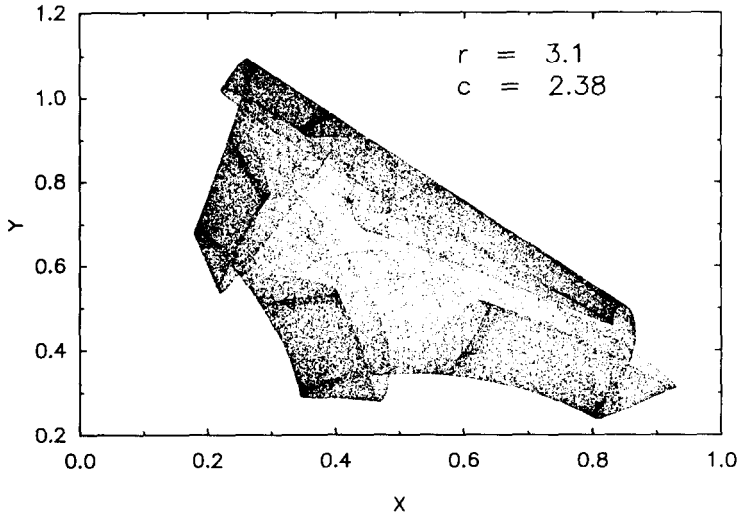

(d)

FIG. 4. (*Continued*)

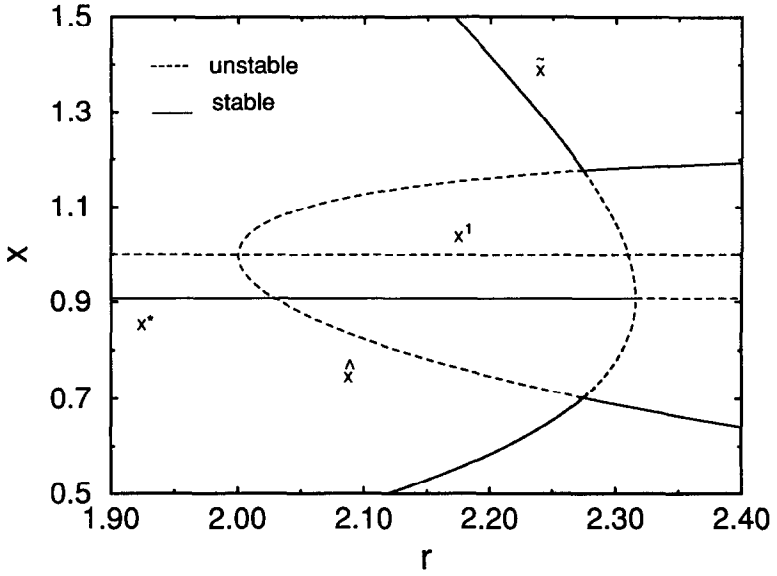

FIG. 5. Bifurcation diagram showing a supercritical flip bifurcation of X^1, a subcritical flip bifurcation of X^*, and a transcritical bifurcation of $\hat{X}$ and $\tilde{X}$ in model (7). Prey numbers are plotted for $c = 1.1$ and various values of the parameter r.

All of the order-2^n cycles of this period-doubling sequence reside on the prey axis. Since X^1 was already a saddle point, they are all unstable.

At the same time, the stable fourth-quadrant 2-cycle,

$$\tilde{X} = \{\tilde{X}_1, \tilde{X}_2\} = \{(x_1, y_1), (x_2, y_2)\}, \tag{13a}$$

$$x_1 = \frac{r - c(r+2) + [r(c+1)(4c-3r+cr)]^{1/2}}{2c(c-r)}, \tag{13b}$$

$$y_1 = \frac{1 + r(1-x_1)}{c} - \frac{1}{c^3(x_1)^2}, \tag{13c}$$

$$x_2 = \frac{r - c(r+2) - [r(c+1)(4c-3r+cr)]^{1/2}}{2c(c-r)}, \tag{13d}$$

$$y_2 = \frac{1 + r(1-x_2)}{c} - \frac{1}{c^3(x_2)^2}, \tag{13e}$$

moves into the first quadrant through $\hat{X}$, exchanging stability with it in a transcritical bifurcation. Both X^* and the prey-axis 2-cycle $\hat{X}$ are now

stable. The existence of multiple stable states in nature is a topic of some debate [7,29,36,40–42]. However, this model clearly allows for their existence. At one attractor, the predator coexists with the prey; at the other, the predator is absent. The stable manifolds of the saddle-like 2-cycle $\tilde{X}$ appear to separate the basins of attraction. Finally, as the boundary (11) is crossed, $\tilde{X}$ collides with X^*. $\tilde{X}$ is destroyed and X^* becomes unstable—via a *subcritical* flip bifurcation—leaving $\hat{X}$, and extinction of the predator, as the only alternative (see Figure 6).

For larger values of c, larger values of r are required to violate (11). Therefore, X^1 will have gone through more than one period doubling by the time X^* becomes unstable, and the prey-axis attractor will be of higher order $(4, 8, 16, \ldots)$ than 2. If $r > 2.57$ when the subcritical flip bifurcation occurs, the dynamics on the prey axis will be chaotic [26]. In general, trajectories will approach the prey axis rapidly. However, for some initial conditions there is a long transient, leading to the fountain phenomenon of Hadeler and Gerstmann [11] (Figure 7). If $r > 3$, the logistic map is no longer invariant on the interval $(0, 4/3)$ and trajectories will diverge to infinity.

5. AN APPLICATION OF CENTER MANIFOLD THEORY

To formally ascertain the (sub- vs. supercritical) nature of the flip bifurcation that occurs as inequality (11) is violated, we would like to apply the following proposition put forward by Whitley [45] concerning a local bifurcation of a one-parameter family of one-dimensional maps, $(\mu, x) \to F_\mu(x)$:

PROPOSITION 1 (Subcritical Flip Bifurcation)

Let $F\colon \mathbb{R} \times \mathbb{R} \to \mathbb{R}$ *be a one-parameter family of* C^3 *maps satisfying*

$$(1)\quad F(\mu_c, 0) = 0 \qquad \textit{and} \qquad (2)\quad \frac{\partial F}{\partial x}(\mu_c, 0) = -1.$$

Then there is a unique branch of fixed points $x(\mu)$ *for* μ *near* μ_c *with* $x(\mu_c) = 0$. *If the eigenvalue* $\lambda(\mu) = (\partial F/\partial x)(x(\mu), \mu)$ *satisfies*

$$(3)\quad \frac{d\lambda}{d\mu}(\mu_c) < 0 \qquad \textit{and also} \qquad (4)\quad \frac{\partial^3 F^2}{\partial x^3}(\mu_c, 0) > 0,$$

then there are intervals (μ_1, μ_c) *and* (μ_c, μ_2) *and* $\epsilon > 0$ *such that*

(i) *If* $\mu \in (\mu_1, \mu_c)$, *then* F_μ *has one stable fixed point and one unstable orbit of period* 2 *in* $(-\epsilon, \epsilon)$.

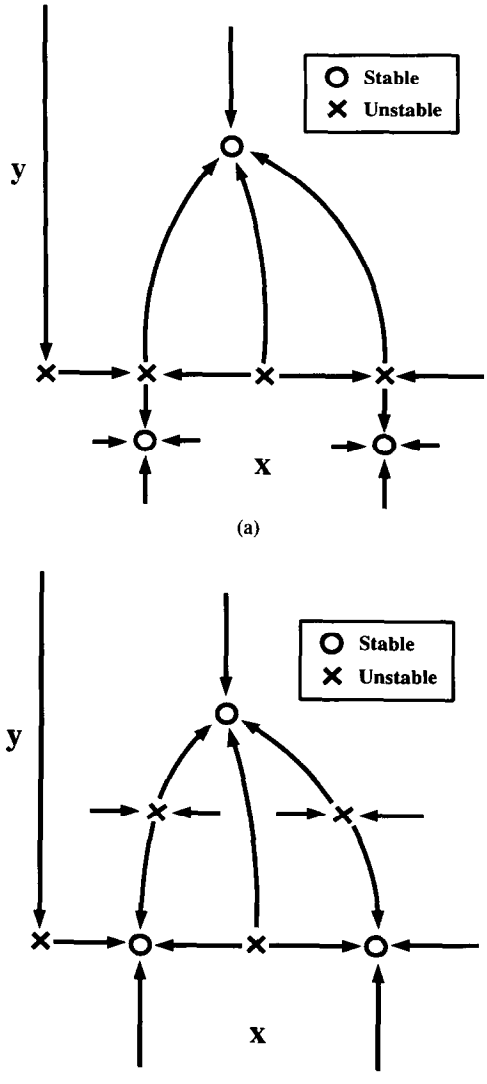

FIG. 6. Schematic phase portraits of model (7) for $c \approx 1.1$ and r increasing through the boundary SF in Figure 1. (a) Before the transcritical bifurcation between $\tilde{X}$ and $\hat{X}$, the only attractor in the first quadrant is the stable fixed point X^*. (b) Just after the transcritical bifurcation, there are two attractors in the first quadrant: X^* and the 2-cycle on the x axis, $\hat{X}$. (c) After the subcritical flip bifurcation of X^*, the predator suffers a population collapse, and trajectories are drawn to the 2-cycle $\hat{X}$.

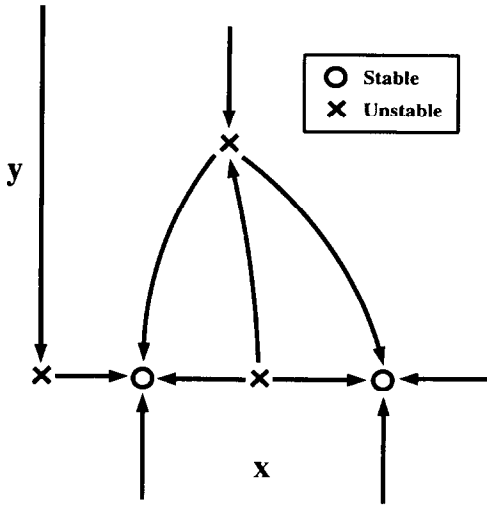

(c)

FIG. 6. *(Continued)*

(ii) *If* $\mu \in (\mu_c, \mu_2)$, *then* $F_\mu^2 = F_\mu \circ F_\mu$ *has a single fixed point in* $(-\epsilon, \epsilon)$ *that is an unstable fixed point of* F_μ.

Of course, we are concerned with a two-dimensional system of difference equations, and so the proposition does not apply directly. However, by applying a technique from center manifold theory [6], we can reduce the dimension of the system to 1, for μ near μ_c and X near X^*.

First, we make the change of variables

$$u_t = x_t - 1/c, \tag{14a}$$

$$v_t = y_t - r(c-1)/c \tag{14b}$$

in system (7). This translates the fixed point X^* to the origin of the (u, v) coordinate plane; system (7) becomes

$$u_{t+1} = f(u_t, v_t) = -ru_t^2 + \left(\frac{c - r - c^2 v_t}{c}\right) u_t - v_t, \tag{15a}$$

$$v_{t+1} = g(u_t, v_t) = \left(\frac{c^2 v_t + r(c-1)}{c}\right) u_t + v_t. \tag{15b}$$

Near $u^* = 0$, $v^* = 0$, $r = 4c/(3-c)$ we assume that there is a center

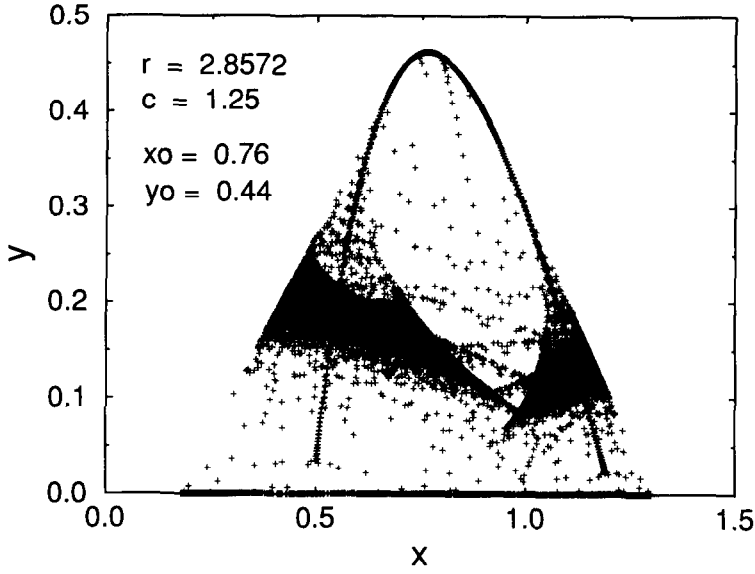

FIG. 7. The fountain phenomenon (cf. Hadeler and Gerstmann [11]). After the subcritical flip bifurcation of X^*, most trajectories are rapidly drawn down to an attractor on the x axis. However, some trajectories experience a long transient that appears as a shower in the phase plane. In this instance, a single trajectory based at ($x_0 = 0.76$, $y_0 = 0.44$) was followed for 50,000 iterations.

manifold of the form

$$v_t = h(u_t) = \alpha u_t + \beta u_t^2 + \gamma u_t^3 + O(u_t^4). \tag{16}$$

Substituting this expression into (15b), we obtain the relation

$$h(u_{t+1}) = g(u_t, h(u_t)). \tag{17}$$

But u_{t+1} can be written as

$$u_{t+1} = f(u_t, h(u_t)), \tag{18}$$

by Equations (15a) and (16). Combining (17) and (18) yields

$$h(f(u_t, h(u_t))) = g(u_t, h(u_t)). \tag{19}$$

By equating coefficients of powers of u_t, we produce the coefficients α, β,

and γ in the power series for h. These have been calculated and are presented in the appendix.

Now, with an expression for $h(u_t)$ in hand, we study the reduced system (18),

$$u_{t+1} = \left(1 - \frac{r}{c} - \alpha\right)u_t - (r + \alpha c + \beta)u_t^2 - (\beta c + \gamma)u_t^3 - \gamma c u_t^4. \tag{20}$$

For

$$\mu = r, \qquad \mu_c = r_c = \frac{4c}{3-c}, \qquad \text{and} \qquad F = f, \tag{21}$$

we have checked the conditions of Proposition 1, and they are satisfied. This implies that the bifurcation is indeed subcritical. Figure 8 shows $f \circ f(u_t, h(u_t))$ before and after the subcritical flip bifurcation.

Note that in the expansion for h it is necessary to keep terms of up to third order in u_t because the fourth condition in Proposition 1 concerns the coefficient of the cubic term in $F \circ F$. It should be emphasized that in the preceding analysis we have held c constant in order to avoid any codimension-2 bifurcations.

6. OTHER MODELS

The presence of a subcritical flip bifurcation is not unique to model (7). In fact, we have found subcritical flip bifurcations in at least three other models:

$$N_{t+1} = N_t \exp\left[r\left(1 - \frac{N_t}{K}\right) - eP_t\right], \tag{22a}$$

$$P_{t+1} = bN_t P_t; \tag{22b}$$

$$N_{t+1} = N_t \exp\left[r\left(1 - \frac{N_t}{K}\right) - eP_t\right], \tag{23a}$$

$$P_{t+1} = N_t\left[1 - \exp(-eP_t)\right]; \tag{23b}$$

and

$$N_{t+1} = N_t + rN_t\left(1 - \frac{N_t}{K}\right) - \frac{eN_t P_t}{N_t + A}, \tag{24a}$$

$$P_{t+1} = \frac{bN_t P_t}{N_t + A}. \tag{24b}$$

Model (22) replaces the logistic prey growth and mass-action functional

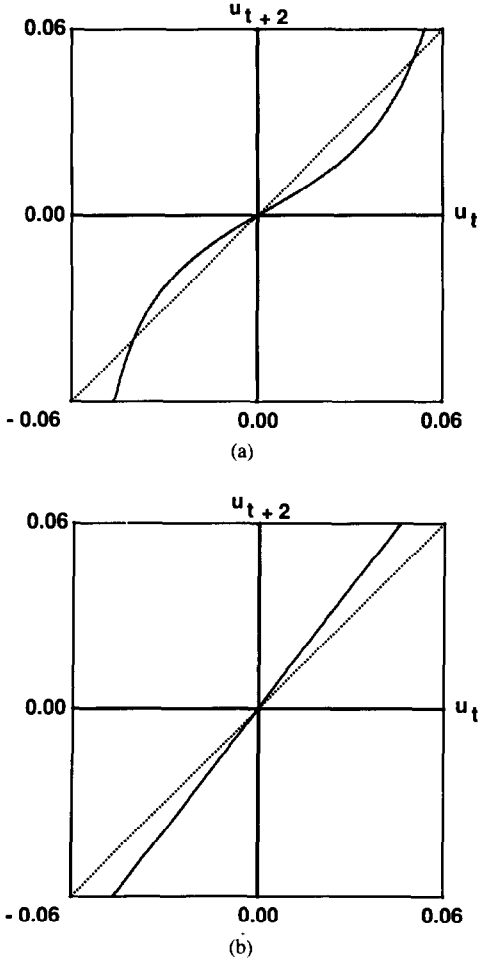

FIG. 8. Plots of $f \circ f(u_t, h(u_t))$. (a) Just before the subcritical flip bifurcation ($r = 3.7$, $\alpha = -0.696884$, $\beta = -10.0029$, $\gamma = 155.033$), there is a stable fixed point and an unstable 2-cycle. (b) After the bifurcation ($r = 4.2$, $\alpha = -0.651669$, $\beta = -3.17159$, $\gamma = 0.690623$), the 2-cycle has disappeared and the fixed point has become unstable. In both cases, $c = 1.5$.

response of model (4) with a Ricker curve [37]. It has been used by Kot [18, 19] and Kot and Schaffer [20] as the descriptor of growth in discrete-time growth-dispersal models. Converting it to a dimensionless form by the transformations

$$x_t = N_t/K, \qquad y_t = eP_t/r, \qquad \text{and} \qquad c = bK \tag{25}$$

yields

$$x_{t+1} = x_t \exp\left[r(1 - x_t - y_t)\right], \tag{26a}$$

$$y_{t+1} = cx_t y_t. \tag{26b}$$

This model possesses a coexistence equilibrium at the point

$$x^* = \frac{1}{c}, \qquad y^* = \frac{c-1}{c}. \tag{27}$$

The linearization of (26) about (27) is identical to (8), and so the stability region for the coexistence equilibrium is again given by the inequalities (10) and (11).

An advantage of this model over (7) is that it maintains first-quadrant invariance. However, the exponential function makes the center manifold calculations harder. Because the system of equations

$$x_{t+2} = x_t, \tag{28a}$$

$$y_{t+2} = y_t \tag{28b}$$

is now transcendental, we are also prevented from obtaining a closed-form expression for the unstable 2-cycle responsible for the subcritical flip bifurcation. However, numerical experiments show that such a bifurcation does occur, with a resultant crash in the predator's population.

Model (23), due to Beddington et al. [4], arises in the study of host–parasitoid interactions. It is an extension of Nicholson and Bailey's model [34, 35] and incorporates the effects of density dependence among the prey. It can be nondimensionalized to

$$x_{t+1} = x_t \exp\left[r(1 - x_t) - y_t\right], \tag{29a}$$

$$y_{t+1} = cx_t\left[1 - \exp(-y_t)\right]. \tag{29b}$$

A linear stability analysis near the unique coexistence equilibrium of (29) produces the stability region shown in Figure 9. Numerical simulations show that the flip bifurcation is subcritical. In this instance, the parasitoid goes extinct.

System (24) is a special case of a model studied by Hadeler and Gerstmann [11]. It is a variant on and a discretization of the system proposed by Rosenzweig [39]; it incorporates a Type II functional response

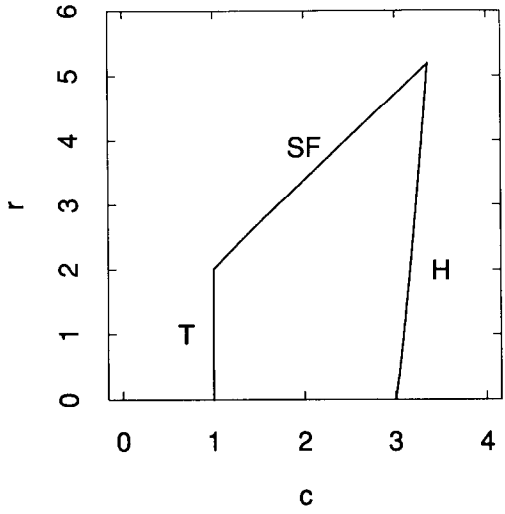

FIG. 9. The region of the parameter plane corresponding to the stability of the coexistence equilibrium X^* of model (29). X^* loses its stability via a transcritical, subcritical flip, or Hopf bifurcation as the boundaries labeled **T**, **SF**, or **H** are traversed.

[15]. One dimensionless form of (24) is

$$x_{t+1} = (r+1)x_t - rx_t^2 - \frac{cx_t y_t}{x_t + \gamma}, \tag{30a}$$

$$y_{t+1} = \frac{cx_t y_t}{x_t + \gamma}. \tag{30b}$$

Figure 10 depicts the stability region, in the (c, r) parameter plane, for the equilibrium

$$x^* = \frac{\gamma}{c-1}, \qquad y^* = rx^*(1-x^*), \tag{31}$$

in the case $\gamma = 1$. The region looks similar for other values of γ.

Hadeler and Gerstmann [11] may have been aware of this subcritical flip bifurcation. In particular, they note the existence of an unstable 2-cycle in the neighborhood of the stable equilibrium of coexistence.

7. DISCUSSION

Supercritical flip bifurcations frequently occur in maps of the interval. This is the situation, for example, in the logistic map and Ricker curve.

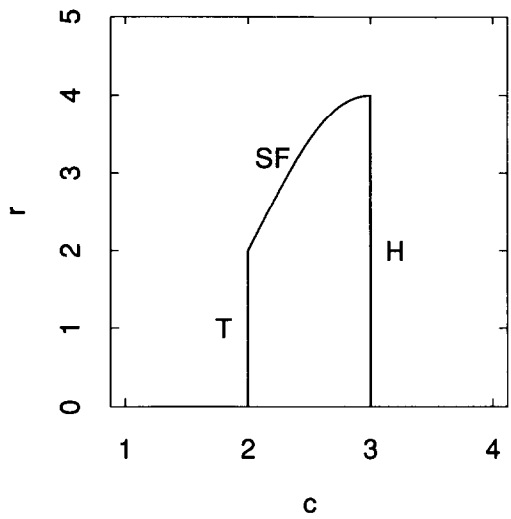

FIG. 10. The region of the parameter plane corresponding to the stability of the coexistence equilibrium X^* of model (30) for $\gamma = 1$. X^* loses its stability via a transcritical, subcritical flip, or Hopf bifurcation as the boundaries labeled **T**, **SF**, or **H** are traversed.

However, Allwright [1] has pointed out that this situation is not generic, even for the "one-hump functions" that one commonly finds in population ecology. He gives as examples

$$x_{t+1} = F(x_t) = x_t \exp\left[2r(1 - x_t)\right] \tag{32}$$

and

$$x_{t+1} = \hat{F}(x_t) = g(rx_t)/g(r), \tag{33a}$$

$$g(u) = u\left\{\exp\left[2(1-u)\right] - (u-1)^3 \exp\left[-3(u-1)^2\right]\right\}. \tag{33b}$$

Although F and $\hat{F}$ have nearly the same shape (Figure 11), at $r = 1$ the former exhibits a supercritical flip bifurcation whereas the later exhibits a subcritical flip bifurcation. As Whitley [45] shows, this can be attributed to the fact that (32) has a Schwarzian derivative,

$$SF(x) = \frac{F'''(x)}{F'(x)} - \frac{3}{2}\left(\frac{F''(x)}{F'(x)}\right)^2, \tag{34}$$

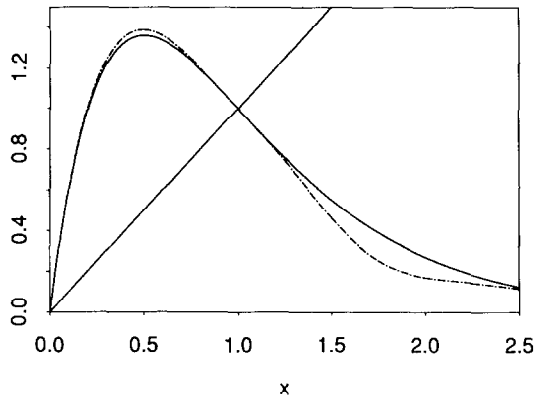

FIG. 11. An example of superficially similar unimodal maps with different bifurcation behaviors. $F(x)$ (solid line) has a supercritical flip bifurcation, whereas $\hat{F}(x)$ (broken line) has a subcritical flip bifurcation. Each is plotted at $r = 1$. (After Allwright [1].)

which is negative at $r = 1$, $x = 1$, whereas the opposite is true for (33). If the Schwarzian derivative, evaluated at the fixed point and the bifurcation value of the parameter, is negative (positive), then a subcritical (supercritical) bifurcation is impossible. This provides a quick test that will reveal the criticality of a flip bifurcation.

When predator and prey interact, the situation is more complicated. We must first reduce the system to one dimension via center manifold theory. Ordinarily this would be considered tedious. However, with the increasing availability of symbolic manipulators it is, in fact, reasonable.

Our own investigation suggests that subcritical flip bifurcations are not to be dismissed out of hand. In at least four instances, the four models discussed in this paper, prey alone exhibit supercritical flip bifurcations whereas the corresponding predator–prey system exhibits a subcritical bifurcation. For each model, a small increase in the growth rate of the prey leads to a radical change in the dynamics of the community. The consequences of this are especially dire: the predator is driven to extinction (cf. [29], [39]).

Finally, we note that subcriticality is not restricted to flip bifurcations or to difference equations. Guckenheimer et al. [9] and Levin [23] have observed a subcritical bifurcation associated with strong resonance in a simple age-structured model, whereas Lauwerier and Metz [22] have analyzed subcritical Hopf bifurcations in host–parasitoid models. In turn, Rinaldi et al. [38] have observed subcritical flip bifurcations in the Poincaré map of a system of differential equations that model a seasonally perturbed predator–prey community.

It is a pleasure to thank Celeste Berg, Eric Funasaki, Mark Lewis, Therese Mar, Mike McCann, and Rebecca Tyson for suggestions and / or discussions. We are also grateful to the Department of Energy (DE-FG06-90ER61034) and to the National Science Foundation (BSR-8907965) for their support.

APPENDIX

These are the coefficients in the expansion of the center manifold (16):

$$\alpha = -\frac{r}{2c} + \frac{1}{2}\left[-4r\left(1-\frac{1}{c}\right) + \frac{r^2}{c^2}\right]^{1/2}, \tag{35a}$$

$$\beta = \frac{6c^3 - 6c^4 + 2c^4 r - c^2 r^2 + (2c^3 - 4c^4 + c^3 r)\left[-4r(1-1/c) + r^2/c^2\right]^{1/2}}{-18c^2 + 18c^3 + 8cr - 14c^2 r + 2c^3 r + 2r^2}, \tag{35b}$$

$$\gamma = \delta/\epsilon\eta, \tag{35c}$$

$$\begin{aligned}\delta = {} & -8c^4 r^5 + c^{11}(-72 + 512r + 88r^2 + 16r^3) \\ & + c^{10}(144 - 1276r - 1096r^2 - 188r^3) \\ & + c^9(-72 + 976r + 2248r^2 + 848r^3) \\ & + c^8(-212r - 1628r^2 - 1156r^3 + 20r^4) \\ & + c^7(404r^2 + 580r^3 - 176r^4) \\ & + c^6(-100r^3 + 220r^4) \\ & + c^5(-76r^4 + 12r^5) \\ & + \left[c^{11}(-348 - 120r - 28r^2) + c^{10}(720 + 784r + 192r^2)\right. \\ & \quad + c^9(-372 - 1100r - 476r^2 + 12r^3) \\ & \quad + c^8(420r + 348r^2 - 72r^3) + c^7(-36r^2 + 140r^3) \\ & \quad \left. + c^6(-68r^3 + 4r^4) - 8c^5 r^4\right]\left[-4r + \frac{4r}{c} + \frac{r^2}{c^2}\right]^{1/2},\end{aligned} \tag{35d}$$

$$\epsilon = (-9c^2 + 9c^3 + 4cr - 7c^2 r + c^3 r + r^2)^2, \tag{35e}$$

$$\begin{aligned}\eta = {} & 16c^2 r - 24c^3 r + 12c^2 r^2 - 4r^3 \\ & - (16c^3 - 12c^2 r + 3cr^2)\left[-4r + \frac{4r}{c} + \frac{r^2}{c^2}\right]^{1/2} \\ & - c^3\left(-4r + \frac{4r}{c} + \frac{r^2}{c^2}\right)^{3/2}.\end{aligned} \tag{35f}$$

REFERENCES

1 D. J. Allwright, Hypergraphic functions and bifurcations in recurrence relations, *SIAM J. Appl. Math.* 34:687–691 (1978).

2 D. G. Aronson, M. A. Chory, G. R. Hall, and R. P. McGehee, A discrete dynamical system with subtly wild behavior, in *New Approaches to Nonlinear Problems in Dynamics*, P. Holmes, Ed., SIAM, Philadelphia, 1980, pp. 339–359.

3 D. G. Aronson, M. A. Chory, G. R. Hall, and R. P. McGehee, Bifurcations from an invariant circle for two-parameter families of maps of the plane: a computer-assisted study, *Commun. Math. Phys.* 83:303–354 (1982).

4 J. R. Beddington, C. A. Free, and J. H. Lawton, Dynamic complexity in predator–prey models framed in difference equations, *Nature* 255:58–60 (1975).

5 J. R. Beddington, C. A. Free, and J. H. Lawton, Characteristics of successful natural enemies in models of biological control of insect pests, *Nature* 273:513–519 (1978).

6 J. Carr, *Applications of Centre Manifold Theory*, Springer-Verlag, New York, 1981.

7 J. H. Connell and W. P. Sousa, On the evidence needed to judge ecological stability or persistence, *Amer. Nat.* 121:789–824 (1983).

8 P. DeBach, *Biological Control by Natural Enemies*, Cambridge Univ. Press, Cambridge, 1974.

9 J. Guckenheimer, G. Oster, and A. Ipaktchi, The dynamics of density dependent population models, *J. Math. Biol.* 4:101–147 (1977).

10 I. Gumowski and C. Mira, *Recurrences and Discrete Dynamic Systems*, Springer-Verlag, New York, 1980.

11 K. P. Hadeler and I. Gerstmann, The discrete Rosenzweig model, *Math. Biosci.* 98:49–72 (1990).

12 M. P. Hassell, *The Dynamics of Arthropod Predator - Prey Systems*, Princeton Univ. Press, Princeton, N.J., 1978.

13 M. P. Hassell, Patterns of parasitism by insect parasitoids in patchy environments, *Ecol. Entomol.* 7:365–377 (1982).

14 M. Henon, Numerical explorations of Hamiltonian systems, in *Chaotic Behavior of Deterministic Systems*, G. Iooss, R. H. G. Helleman, and R. Stora, Eds., North-Holland, Amsterdam, 1983, pp. 54–170.

15 C. S. Holling, The components of predation as revealed by a study of small-mammal predation of the European pine sawfly, *Can. Entomol.* 41:293–320 (1959).

16 G. Iooss, *Bifurcation of Maps and Applications*, North-Holland, Amsterdam, 1979.

17 E. I. Jury, *Inners and Stability of Dynamic Systems*, Wiley, New York, 1974.

18 M. Kot, Diffusion-driven period-doubling bifurcations, *BioSystems* 22:279–287 (1989).

19 M. Kot, Discrete-time travelling waves: ecological examples, *J. Math. Biol.* 30:413–436 (1992).

20 M. Kot and W. M. Schaffer, Discrete-time growth-dispersal models, *Math. Biosci.* 80:109–136 (1986).

21 H. A. Lauwerier, Two-dimensional iterative maps, in *Chaos*, A. V. Holden, Ed., Princeton Univ. Press, Princeton, N.J., 1986, pp. 58–95.

22 H. A. Lauwerier and J. A. Metz, Hopf bifurcation in host-parasitoid models, *IMA J. Math. Appl. Med. Biol.* 3:191-210 (1986).
23 S. Levin, Age-structure and stability in multiple-age spawning populations, in *Renewable Resource Management*, T. L. Vincent and J. M. Skowronski, Eds., Springer-Verlag, Heidelberg, 1981, pp. 21-45.
24 S. H. Levine, Discrete time modeling of ecosystems with applications in environmental enrichment, *Math. Biosci.* 24:307-317 (1975).
25 A. J. Lotka, *Elements of Physical Biology*, Williams & Wilkins, Baltimore, 1925.
26 R. M. May, Biological populations with nonoverlapping generations: stable points, stable cycles, and chaos, *Science* 186:645-647 (1974).
27 R. M. May, Biological populations obeying difference equations: stable points, stable cycles, and chaos, *J. Theor. Biol.* 51:511-524 (1975).
28 R. M. May, Simple mathematical models with very complicated dynamics, *Nature* 261:459-467 (1976).
29 R. M. May, Thresholds and breakpoints in ecosystems with a multiplicity of stable states, *Nature* 269:471-477 (1977).
30 J. Maynard Smith, *Mathematical Ideas in Biology*, Cambridge Univ. Press, Cambridge, 1968.
31 J. Maynard Smith, *Models in Ecology*, Cambridge Univ. Press, Cambridge, 1974.
32 H. C. Morris, E. E. Ryan, and R. K. Dodd, Snap-back repellers and chaos in a discrete population model with delayed recruitment, *Nonlin. Anal.* 7:571-621 (1983).
33 W. W. Murdoch and A. Stewart-Oaten, Aggregation by parasitoids and predators: effects on equilibrium and stability, *Amer. Nat.* 134:288-310 (1989).
34 A. J. Nicholson, The balance of animal populations, *J. Anim. Ecol.* 2:132-178 (1933).
35 A. J. Nicholson and V. A. Bailey, The balance of animal populations, *Proc. Zool. Soc. Lond.*, 1935, pp. 551-598.
36 C. H. Peterson, Does a rigorous criterion for environmental identity preclude the existence of multiple stable points?, *Amer. Nat.* 124:127-133 (1984).
37 W. E. Ricker, Stock and recruitment, *J. Fish. Res. Bd. Can.* 11:559-623 (1954).
38 S. Rinaldi, S. Muratori, and Y. Kuznetsov, Multiple attractors, catastrophes, and chaos in seasonally perturbed predator-prey communities, *Bull. Math. Biol.* (in press).
39 M. Rosenzweig, Paradox of enrichment: destabilization of exploitation ecosystems in ecological time, *Science* 171:385-387 (1971).
40 W. P. Sousa and J. H. Connell, Further comments on the evidence for multiple stable points in natural communities, *Amer. Nat.* 125:612-615 (1985).
41 J. P. Sutherland, Multiple stable points in natural communities, *Amer. Nat.* 108:859-873 (1974).
42 J. P. Sutherland, Perturbations, resistance, and alternative views of the existence of multiple stable points in nature, *Amer. Nat.* 136:270-275 (1990).
43 V. Volterra, *Leçons sur la Theorie Mathematique de la Lutte pour la Vie*, Gauthier-Villars, Paris, 1931.
44 S. J. Walde and W. W. Murdoch, Spatial density dependence in parasitoids, *Ann. Rev. Entomol.* 33:441-466 (1988).
45 D. Whitley, Discrete dynamical systems in dimensions one and two, *Bull. Lond. Math. Soc.* 15:177-217 (1983).